

Depolarisation rates of Ca II s, p and d levels by isotropic collisions with hydrogen atoms

B. Kerkeni*, A. Spielfiedel, and N. Feautrier

Laboratoire d'Étude du Rayonnement et de la Matière en Astrophysique, CNRS FRE 2460 – LERMA, Observatoire de Paris, Section de Meudon, 92195 Meudon, France

Received 30 July 2002 / Accepted 21 January 2003

Abstract. Multipole relaxation and transfer rates of the $4s^2S$, $3d^2D$ and $4p^2P$ states of Ca II due to isotropic collisions with neutral hydrogen atoms are calculated. Evaluation of these rates have been carried out using accurate ab initio potential energy curves. The collisional T-matrix elements required for these calculations have been evaluated in a quantum mechanical description including fine structure splitting. Analytical expressions of all the rates valid for $200\text{ K} \leq T \leq 10\,000\text{ K}$ are given.

Key words. Sun: atmosphere – atomic processes – line: formation – polarization

1. Introduction

The linearly polarised solar limb spectrum that is due to scattering processes on the Sun is currently known as “the second solar spectrum” (Stenflo & Keller 1997; Stenflo et al. 2000; Stenflo 2001; Gandorfer 2000, 2002). It is full of exciting linear polarisation signatures whose explanation has motivated a number of important theoretical investigations on scattering polarisation and the Hanle effect (Trujillo Bueno & Landi Degl’Innocenti 1997; Landi Degl’Innocenti 1998, 1999; Trujillo Bueno 1999, 2001; Manso Sainz & Trujillo Bueno 2001; Casini et al. 2002; Trujillo Bueno et al. 2002a,b; Manso Sainz & Landi Degl’Innocenti 2002; Kerkeni & Bommier 2002). Such linear polarisation signatures in spectral lines are of great interest for the investigation of the physical conditions and magnetic fields in the solar atmosphere and have a great diagnostic potential for future investigations in other astrophysical contexts.

Among the most interesting enigmatic features of the second solar spectrum are the observed fractional polarisation amplitudes in the IR triplet of ionized calcium (see the Q/I observations of Stenflo et al. 2000 and the full Stokes-vector observations of Dittmann et al. 2001).

The explanation of such enigmatic observational results in the IR triplet of ionised calcium was given by Manso Sainz & Trujillo Bueno (2001) and by Trujillo Bueno & Manso Sainz (2001), who were able to formulate and solve the multilevel scattering polarisation problem including the Hanle effect operating in a realistic

multilevel model of ionized calcium. Although these authors include the effect of elastic and inelastic collisions, they use, for the collisions with atomic hydrogen, rates obtained from the long range van der Waals interaction (Lamb & ter Haar 1971). This approximation may underestimate the collisional rates; so it is of considerable importance to provide new values obtained via the application of quantum chemistry methods like those applied by Kerkeni et al. (2000) and Kerkeni (2002) in previous papers of this series (hereafter Papers I and II, respectively).

The aim of this paper is to extend such calculations to the atomic levels involved in the formation of the H and K lines and of the IR triplet of ionized calcium.

The present paper is organized as follows. Section 2 focuses on the calculation of molecular potential energy curves, while Sect. 3 considers the dynamical calculations. Finally, the main results are given and summarized in Sects. 4 and 5, respectively.

2. Ab initio potentials for Ca⁺H

The potential energy curves were obtained by quantum chemistry methods (see Paper II for the description of the theoretical concepts) using the MOLPRO package¹. The approach is that previously used by Leininger et al. (2000) to calculate the NaH potential energy curves. The Ca II ion is treated as a one-electron system in a pseudopotential

¹ MOLPRO is a package of ab initio programs written by H.-J. Werner and P. J. Knowles, with contributions from J. Almlöf, R. D. Amos, A. Berning, M. J. O. Deegan, F. Eckert, S. T. Elbert, C. Hampel, R. Lindh, W. Meyer, A. Nicklass, K. Peterson, R. Pitzer, A. J. Stone, P. R. Taylor, M. E. Mura, P. Pulay, M. Schuetz, H. Stoll, T. Thorsteinsson, and D. L. Cooper.

Send offprint requests to: B. Kerkeni,
e-mail: boutheina.kerkeni@chem.ox.ac.uk

* Present address: Physical and Theoretical Chemistry Laboratory, Oxford University, South parks road, Oxford OX1 3QH, UK.

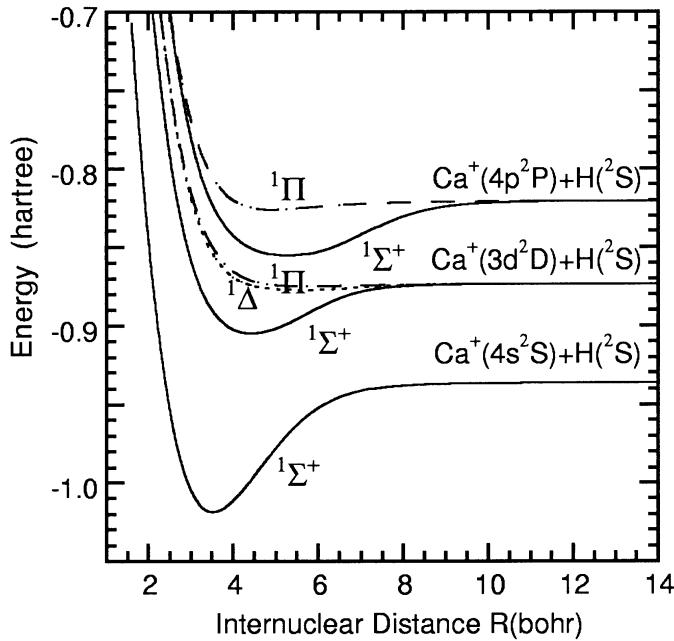


Fig. 1. Singlet potential energy curves for Ca⁺H.

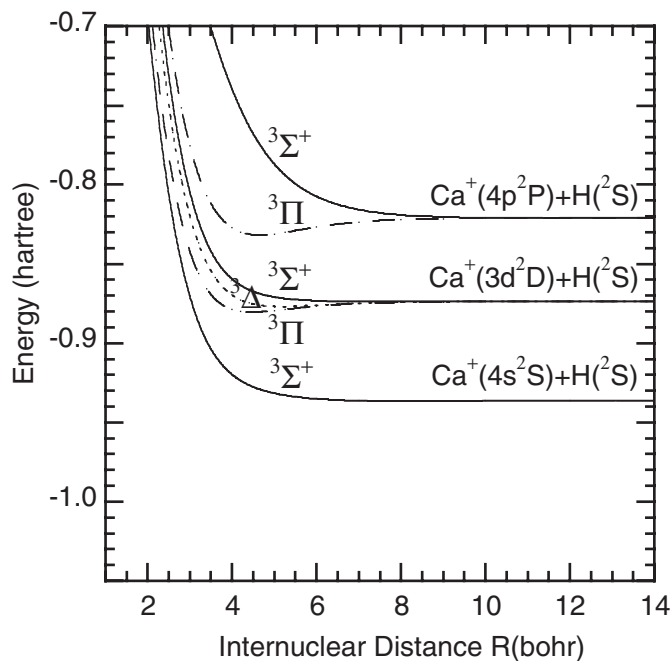


Fig. 2. Triplet potential energy curves for Ca⁺H.

(Fuentealba et al. 1985) and the core-valence correlation energy is estimated consistently with the core-polarisation potential approach (Müller et al. 1984). A large Gaussian basis set was used. The hydrogen basis is (4s, 3p, 2d) from a quintuple-zeta basis set of Dunning (1989). For the calcium ion, the basis includes the (9s, 7p, 6d) functions of (Czuchaj et al. 2000) contracted to [7s, 6p, 6d] and augmented with an *f* function. With this approach, the energy levels up to the Ca⁺ (5p²P) state are in very good agreement (Czuchaj et al. 2000) with the experimental energy levels. The electronic states correlated to the three lower asymptotes were calculated from a

Multi Configuration Self Consistent Field (MCSCF) approach in the (1σ – 9σ, 1π – 4π, 1δ – 2δ) active space, followed by a Configuration Interaction (CI) calculation including all single and double excitations from the MCSCF wave function (see Paper II).

The singlet and triplet symmetry states are shown in Figs. 1 and 2 respectively. The main characteristic of these potential energy curves is the presence of a large well in the ¹Σ⁺ states due to the contribution of the ionic configuration Ca²⁺H⁻ in the region of internuclear distances [4 – 12a₀] where depolarising rates are sensitive. Fair agreement is obtained with the extensive calculations of Mc Farland et al. (1982) for the CaH⁺ X¹Σ⁺ and a³Σ⁺ states.

3. Dynamics

3.1. Close coupling equations

The potential energy curves described above were used to compute depolarising and transfer cross sections. Fully quantal close-coupling studies of the system Ca⁺-H were performed using the formulation given by Mies (1973), generalized by Launay & Roueff (1977) and previously used for calculations of depolarising rates of Na I, Ca I, Sr I and Mg I by Kerkeni (2002).

Since the fine structure splittings are relatively important (222.89 cm⁻¹ for ²P_{1/2-3/2} and 60.69 cm⁻¹ for ²D_{3/2-5/2}) they were taken into account in the close-coupling calculations.

The upper atomic states of the infrared triplet have *J* = 1/2 and 3/2, while the lower levels have *J* = 3/2 and 5/2. The emitted transition *J* = 3/2 → 3/2 produces the 8498 Å line, the *J* = 3/2 → 5/2 transition the 8542 Å line, the 1/2 → 3/2 transition the 8662 Å line. The H and K lines occur at 3968 Å and 3933 Å; their lower state has *J* = 1/2, the upper states *J* = 1/2 and *J* = 3/2 are common to the upper states of the infrared triplet.

The radiating atom with angular momentum *J* collides with an H atom with angular momentum *j*₂. We couple *J* and *j*₂ to obtain the total angular momentum *j* of the two atoms. Owing to the invariance of the interaction potential *V* under rotations of the total system, the total angular momentum *J*^T = *j* + *l* and its space fixed projection *M*^T are conserved during the collision. It is convenient to use scattering channel states |*Jj*₂*j**l**J*^T⟩ which describe the asymptotic fragments with relative angular momentum *l*. The total wave function is expanded in terms of these channel states; the expansion coefficients are the radial amplitudes *F*_{*Jj*₂*j**l**J*^T} which satisfy the usual coupled radial equations (Spielfiedel et al. 1991). This set of equations is always decoupled into two blocks as a result of parity conservation. In the calculations, we have assumed that the H atom remains in its ground ²S state (*L*₂ = 0, *j*₂ = 1/2) and we have neglected collision-induced quenching of the other *L* states of the radiating atom. The scattering equations were solved subject to boundary conditions which define the T-matrix elements (Spielfiedel et al. 1991). The numerical method used is the Log Derivative Method (Johnson 1977). Convergence was checked in terms of the range and step size of the scattering coordinate in the radial equations.

Table 1. List of angular momenta defining the channel states for a collisional close coupling calculation of an atom in a 2D state perturbed by H ($j_2 = 1/2$).

Parity	$(-)^{J^T}$			$(-)^{J^T+1}$			
	channel number	J	j	ℓ	J	j	ℓ
	1	3/2	1	J^T	3/2	1	$J^T - 1$
	2	3/2	2	$J^T - 2$	3/2	1	$J^T + 1$
	3	3/2	2	J^T	3/2	2	$J^T - 1$
	4	3/2	2	$J^T + 2$	3/2	2	$J^T + 1$
	5	5/2	2	$J^T - 2$	5/2	2	$J^T - 1$
	6	5/2	2	J^T	5/2	2	$J^T + 1$
	7	5/2	2	$J^T + 2$	5/2	3	$J^T - 3$
	8	5/2	3	$J^T - 2$	5/2	3	$J^T - 1$
	9	5/2	3	J^T	5/2	3	$J^T + 1$
	10	5/2	3	$J^T + 2$	5/2	3	$J^T + 3$

Collisional depolarisation occurs both in the ground state ($4s\ ^2S_{1/2}$) and in the excited states ($3d\ ^2D_{3/2}$, $3d\ ^2D_{5/2}$) and ($4p\ ^2P_{1/2}$, $4p\ ^2P_{3/2}$). The excited 2D_J states of the Ca II ion correspond to an electronic angular momentum $L = 2$ and an electronic spin $S = 1/2$, so that the total electronic angular momentum J is $3/2$ or $5/2$. The number ($2N$) of channel states is given by all the possible combinations $|J j_2 j \ell J^T\rangle$, which are obtained as follows: for each value of J , following the selection rules, j takes the values $|J - j_2|, \dots, |J + j_2|$ with $j_2 = 1/2$. The relative motion angular momentum ℓ takes the selective values comprised between $|J^T - j|$ and $|J^T + j|$. We obtain two sets of channel states of opposite parity (see Table 1). For each energy, due to parity decoupling, the calculation of the T^{J^T} collision matrices requires the solution of two independent sets of N coupled equations for a total angular momentum J^T ranging from 3 (due to a condition of non-negative ℓ value) up to a large value (about 700) insuring negligible contributions of larger J^T values (see Table 1). For $\text{Ca}^+(3d\ ^2D)$, the number of coupled equations is $N = 10$ whereas it is $N = 6$ (see Paper II) for $\text{Ca}^+(4p\ ^2P)$. For $\text{Ca}^+(4s\ ^2S)$, a set of $N = 2$ uncoupled equations must be solved.

3.2. Relaxation and transfer rates

Under typical conditions of formation of strong lines in stellar and solar atmospheres, the impact approximation is valid and the interaction of the radiating atomic system with the perturbing gas is given by the frequency-independent depolarisation matrix \hat{g} . This depolarisation matrix can be expressed in terms of collisional amplitudes (Nienhuis 1976) or collision T-matrix elements (Fano 1963). As the internal state distribution of the perturbers and the distribution of relative velocities are isotropic, the collisional depolarisation of the atomic density matrix ρ is fully isotropic. As a consequence, the depolarisation matrix \hat{g} is considerably simplified by using an expansion in T_q^k components of irreducible tensorial sets (Fano 1949, 1954, 1957; Omont 1977; Blum 1981). Owing to the isotropy of the collisional depolarisation, only the multipole components with

the same value of κ and q are coupled, and the depolarisation rate parameters are q independent. For a given L-state, the relaxation equations give the variation of the multipole components $\rho_q^k(J)$ of the atomic density matrix of a given J level in terms of the multipole components of all the J' levels collisionally coupled to J . Hence the depolarisation equations may be written as (see Paper II):

$$\left(\frac{d\rho_q^k(J)}{dt}\right)_{\text{rel}} = -g^k(J)\rho_q^k(J) + \sum_{J' \neq J} g^k(J' \rightarrow J)\rho_q^k(J') \quad (1)$$

$g^k(J' \rightarrow J)$ and $g^k(J)$ are expressed in terms of the cross sections as:

$$g^k(J' \rightarrow J) = n_H \int_0^\infty v f(v) dv \sigma^k(J' \rightarrow J)$$

$$g^k(J) = n_H \int_0^\infty v f(v) dv \sigma^k(J) \quad (2)$$

with:

$$\sigma^k(J' \rightarrow J) = \sum_m (-1)^{J+J'+\kappa+m} (2m+1) \left\{ \begin{matrix} J' & J' & \kappa \\ J & J & m \end{matrix} \right\} B(JJ', m) \quad (3)$$

$$\sigma^k(J) = \Lambda^k(J) + \sum_{J' \neq J} \sigma(J \rightarrow J') \quad (4)$$

$$\Lambda^k(J) = \sum_m \frac{2m+1}{2J+1} \left[1 - (-1)^{2J+\kappa+m} (2J+1) \right. \\ \left. \times \left\{ \begin{matrix} m & J & J \\ \kappa & J & J \end{matrix} \right\} \right] B(JJ; m) \quad (5)$$

and

$$B(JJ'; m) = \frac{\pi}{(2j_2+1)k_B^2} \sum_{j_b j_b'} (2j_b+1)(2j_b'+1) \\ \times \left| \sum_{J^T j^T} \sqrt{(2j+1)(2j'+1)} (-1)^{J+j_2+J^T} \left\{ \begin{matrix} J & j_2 & j \\ \ell & J^T & j_b \end{matrix} \right\} \right. \\ \left. \times \left\{ \begin{matrix} J' & j_2 & j' \\ \ell' & J^T & j_b' \end{matrix} \right\} \left\{ \begin{matrix} J & J' & m \\ j_b' & j_b & J^T \end{matrix} \right\} \left\langle J' j_2 j' \ell' J^T | T | J j_2 j \ell J^T \right\rangle \right|^2. \quad (6)$$

Coefficients $g^k(J' \rightarrow J)$ correspond to collisional transfer of population ($\kappa = 0$), orientation ($\kappa = 1, 3, 5$) and alignment ($\kappa = 2, 4$) from atomic state J' to state J . The transfer rates $g^k(J \rightarrow J')$ and $g^k(J' \rightarrow J)$ are related through (Omont 1977):

$$g^k(J \rightarrow J') = \exp(-(E_J - E_{J'})/k_B T) g^k(J' \rightarrow J) \quad (7)$$

where E_J and $E_{J'}$ are the energies of levels J and J' respectively, k_B is the Boltzman constant and T is the temperature.

The depolarisation cross section $\sigma^k(J)$ is the sum of two terms: $\Lambda^k(J)$ and the fine structure transfer cross sections $\sum_{J' \neq J} \sigma(J \rightarrow J')$. Explicit expressions of the $\Lambda^k(J)$ and $\sigma^k(J' \rightarrow J)$ for $J = 1/2$ and $3/2$ in terms of the Grawert parameters B (see Paper II for definition of B) were given by Reid (1973) and Kerkeni (2002) respectively. Expressions for $J = 5/2$ are given in Appendix A. The fine structure transfer cross section is also given as a linear combination of the Grawert parameters B :

$$\sigma(J' \rightarrow J) = \sum_m \frac{2m+1}{2J'+1} B(JJ'; m). \quad (8)$$

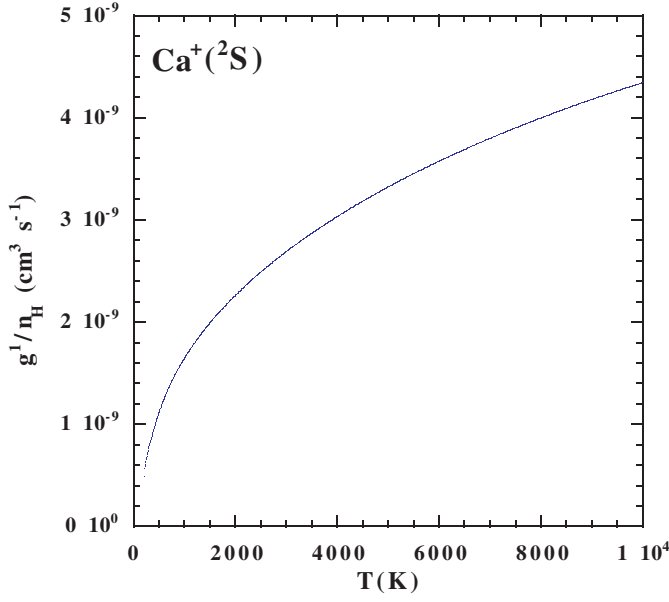


Fig. 3. Relaxation rate g^1/n_H ($\text{cm}^3 \text{s}^{-1}$) as a function of temperature T (K).

The usual fine structure transfer rate is defined by:

$$g(J' \rightarrow J) = n_H \int_0^\infty v f(v) dv \sigma(J' \rightarrow J) \quad (9)$$

and $g^0(J \rightarrow J')$ is proportional to $g(J \rightarrow J')$:

$$g^0(J \rightarrow J') = \sqrt{\frac{2J+1}{2J'+1}} g(J \rightarrow J'). \quad (10)$$

In Eqs. (2) and (9) $f(v)$ is the Maxwellian distribution of relative velocities v at temperature T .

4. Results

Depolarising rates pertaining to the ground state ($4s \ ^2S_{1/2}$) and the excited states ($3d \ ^2D_{3/2}$, $3d \ ^2D_{5/2}$) and ($4p \ ^2P_{1/2}$, $4p \ ^2P_{3/2}$) have been computed. About twenty five energy values were needed to insure the convergence of the velocity integration of the rates.

Figure 3 shows the orientation depolarising rate g^1 of the 2S state, as function of the temperature. This rate is smaller compared with g^1 of the Na I atom (for Na I at 5000 K: $g^1/n_H = 4.32 \times 10^{-9} \text{ cm}^3 \text{ s}^{-1}$, see Paper I). In Fig. 4 are plotted $g^1(^2P_{1/2})$, $g^\kappa(^2P_{3/2})$ with ($\kappa = 1, 2, 3$), and the fine structure transfer rate $g(1/2 \rightarrow 3/2)$. The most striking feature of the figure is the close variation of the $g^3(^2P_{3/2})$ and $g^1(^2P_{1/2})$ rates; we also note that for the $^2P_{3/2}$ state, $g^1 < g^3 < g^2$ as was the case for Na I (see Paper II).

At a given temperature of 5000 K, the fine structure transfer rate was found to be $4.18 \times 10^{-9} \text{ cm}^3 \text{ s}^{-1}$ which is in good agreement with the value of Monteiro et al. (1988) ($4.21 \times 10^{-9} \text{ cm}^3 \text{ s}^{-1}$) obtained from potentials that include correctly the ionic configuration in the $^1\Sigma^+$ molecular states. This indicates the importance of a correct description of the potentials in the intermediate and large distances. Due to the important role of fine structure splitting during the collisional processes,

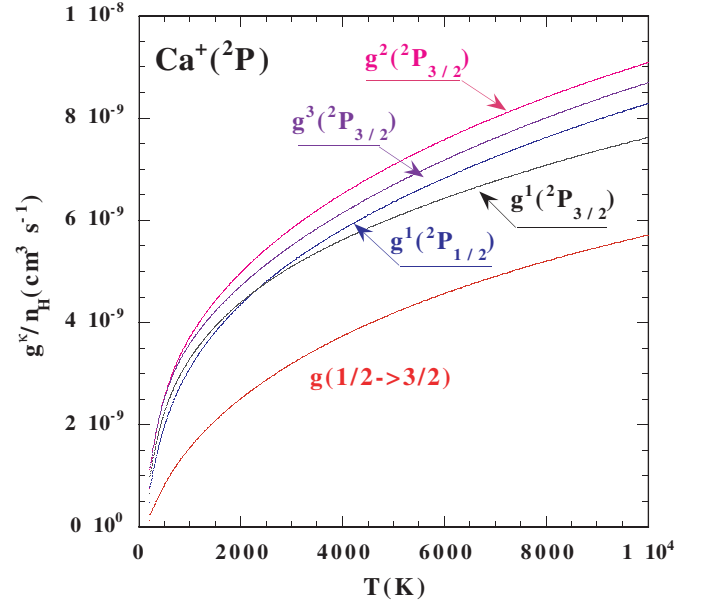


Fig. 4. Fine structure transfer and depolarisation rates g^κ/n_H ($\text{cm}^3 \text{s}^{-1}$) as a function of temperature T (K) for the $\text{Ca}^+(^2P)$.

the fine structure transfer rate is the principal contribution to the $g^\kappa(^2P)$ rates. The orientation transfer rate $g^1(1/2 \rightarrow 3/2)$ (shown separately in Fig. 5) is negative with a magnitude much lower than the $g^\kappa(^2P)$ coefficients.

Considering the 2D coefficients, Figs. 6 and 7 show that the depolarising rates of the $J = 3/2$ level are of the same order of magnitude as those of the $J = 5/2$ level; they are small compared to the 2P coefficients. The same trend in the ordering of the $g^\kappa(^2P_{3/2})$ was found for $g^\kappa(^2D_{3/2})$: $g^1 < g^3 < g^2$. The fine structure transfer rate $g(3/2 \rightarrow 5/2)$ which is the difference between the relaxation rate $g^\kappa(J)$ and the rate corresponding to the $\Lambda^\kappa(J)$ cross section, is given in Fig. 6 and represents also the principal contribution to the $g^\kappa(^2D)$ rates. The collisional transfer rates of orientation and alignment $g^\kappa(3/2 \rightarrow 5/2)$, not shown here, vary between 10^{-11} and $10^{-10} \text{ cm}^3 \text{ s}^{-1}$, consequently their contribution to the statistical equilibrium equations to derive the degree of linear polarisation of the scattered radiation can be neglected.

The variation of the depolarising and transfer rates with the temperature is very smooth. It is found to vary as T^α and is given as follows for $200 \text{ K} \leq T \leq 10000 \text{ K}$ (except for the orientation transfer rate $g^1(1/2 \rightarrow 3/2)$ given for $2500 \text{ K} \leq T \leq 7500 \text{ K}$):

$\text{Ca}^+(^2S)+\text{H}$:

Depolarising rate:

$$J = 1/2$$

$$g^1 = 3.2935 \times 10^{-9} n_H \left(\frac{T}{5000} \right)^{0.451} (\text{s}^{-1}). \quad (11)$$

$\text{Ca}^+(^2P)+\text{H}$:

Depolarising rates:

$$J = 1/2$$

$$g^1 = 6.2873 \times 10^{-9} n_H \left(\frac{T}{5000} \right)^{0.476} (\text{s}^{-1}) \quad (12)$$

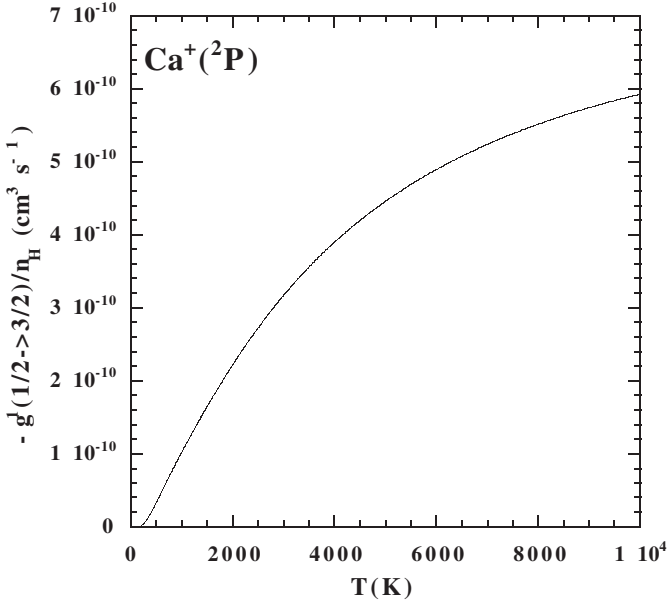


Fig. 5. Transfer rate $-g^{1/2 \rightarrow 3/2}/n_H$ ($\text{cm}^3 \text{s}^{-1}$) as function of temperature T (K) for the $\text{Ca}^+(^2\text{P})$.

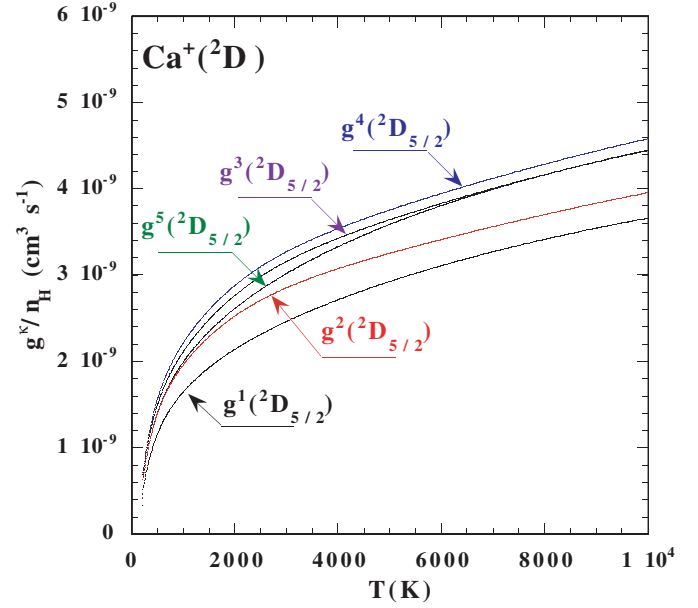


Fig. 7. Relaxation rates g^k/n_H ($\text{cm}^3 \text{s}^{-1}$) as a function of temperature T (K) for the $\text{Ca}^+(^2\text{D})$.

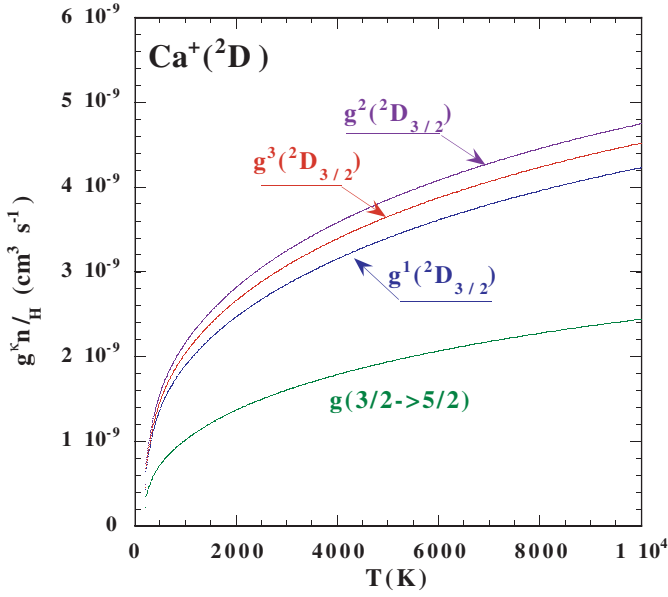


Fig. 6. Fine structure transfer and depolarisation rates g^k/n_H ($\text{cm}^3 \text{s}^{-1}$) as a function of temperature T (K) for the $\text{Ca}^+(^2\text{D})$.

$J = 3/2$

$$\begin{aligned} g^1 &= 6.0059 \times 10^{-9} n_H \left(\frac{T}{5000} \right)^{0.406} \text{ (s}^{-1}\text{)} \\ g^2 &= 7.0291 \times 10^{-9} n_H \left(\frac{T}{5000} \right)^{0.428} \text{ (s}^{-1}\text{)} \\ g^3 &= 6.6772 \times 10^{-9} n_H \left(\frac{T}{5000} \right)^{0.418} \text{ (s}^{-1}\text{)}. \end{aligned} \quad (13)$$

Fine structure and polarisation transfer rates:

$$\begin{aligned} g^0(1/2 \rightarrow 3/2) &= 2.8713 \times 10^{-9} n_H \left(\frac{T}{5000} \right)^{0.642} \text{ (s}^{-1}\text{)} \\ g(1/2 \rightarrow 3/2) &= \sqrt{2} \times g^0(1/2 \rightarrow 3/2) \end{aligned} \quad (14)$$

$$g(3/2 \rightarrow 1/2) = \frac{1}{\sqrt{2}} \times g^0(3/2 \rightarrow 1/2) \quad (15)$$

$$g^1(1/2 \rightarrow 3/2) = -4.3726 \times 10^{-10} n_H \left(\frac{T}{5000} \right)^{0.599} \text{ (s}^{-1}\text{)}. \quad (16)$$

$\text{Ca}^+(^2\text{D})+\text{H}$:

Depolarising rates:

$J = 3/2$

$$\begin{aligned} g^1 &= 3.3700 \times 10^{-9} n_H \left(\frac{T}{5000} \right)^{0.381} \text{ (s}^{-1}\text{)} \\ g^2 &= 3.8120 \times 10^{-9} n_H \left(\frac{T}{5000} \right)^{0.376} \text{ (s}^{-1}\text{)} \\ g^3 &= 3.6154 \times 10^{-9} n_H \left(\frac{T}{5000} \right)^{0.380} \text{ (s}^{-1}\text{)}. \end{aligned} \quad (17)$$

$J = 5/2$

$$\begin{aligned} g^1 &= 2.9078 \times 10^{-9} n_H \left(\frac{T}{5000} \right)^{0.385} \text{ (s}^{-1}\text{)} \\ g^2 &= 3.2387 \times 10^{-9} n_H \left(\frac{T}{5000} \right)^{0.341} \text{ (s}^{-1}\text{)} \\ g^3 &= 3.6143 \times 10^{-9} n_H \left(\frac{T}{5000} \right)^{0.359} \text{ (s}^{-1}\text{)} \\ g^4 &= 3.7318 \times 10^{-9} n_H \left(\frac{T}{5000} \right)^{0.353} \text{ (s}^{-1}\text{)} \\ g^5 &= 3.5506 \times 10^{-9} n_H \left(\frac{T}{5000} \right)^{0.387} \text{ (s}^{-1}\text{)}. \end{aligned} \quad (18)$$

Fine structure and polarisation transfer rates:

$$g^0(3/2 \rightarrow 5/2) = 1.556 \times 10^{-9} n_H \left(\frac{T}{5000} \right)^{0.288} \text{ (s}^{-1}\text{)} \quad (19)$$

$$\begin{aligned} g(3/2 \rightarrow 5/2) &= \frac{\sqrt{6}}{2} \times g^0(3/2 \rightarrow 5/2) \\ g(5/2 \rightarrow 3/2) &= \frac{\sqrt{6}}{3} \times g^0(5/2 \rightarrow 3/2). \end{aligned} \quad (20)$$

5. Discussion and conclusions

In the temperature range $200 \text{ K} \leq T \leq 10\,000 \text{ K}$, the functional form $g(T) = a \times (T/5000)^\alpha$ may be accurately fitted to all g^κ coefficients. The same order of magnitude was found for $g^\kappa(^2\text{S})$ and $g^\kappa(^2\text{D})$ ($a \approx 3 - 4 \times 10^{-9}$) whereas $g^\kappa(^2\text{P})$ was found to be about twice as large.

All rates were found to increase with T , and exponents α to be somewhat L -term dependent (α decreases as L increases). All transfer rates are significantly smaller.

These conclusions also hold for Na I (Paper II). It would be interesting to confirm these trends by studying other atomic systems.

Acknowledgements. The computations were performed on the work stations of the computer center of Observatoire de Paris. The authors acknowledge the referee for comments that improve and clarify the manuscript.

Appendix A: Definition of the multipole depolarisation and transfer cross sections in the $^2\text{D}_J$ excited states

We report here our calculated Λ^κ for $J = \frac{5}{2}$:

$$\begin{aligned}
 \Lambda^0\left(\frac{5}{2}\right) &= 0 \\
 \Lambda^1\left(\frac{5}{2}\right) &= \frac{2}{35}B\left(\frac{55}{22}; 1\right) + \frac{2}{7}B\left(\frac{55}{22}; 2\right) + \frac{4}{5}B\left(\frac{55}{22}; 3\right) \\
 &\quad + \frac{12}{7}B\left(\frac{55}{22}; 4\right) + \frac{22}{7}B\left(\frac{55}{22}; 5\right) \\
 \Lambda^2\left(\frac{5}{2}\right) &= \frac{6}{35}B\left(\frac{55}{22}; 1\right) + \frac{3}{4}B\left(\frac{55}{22}; 2\right) + \frac{33}{20}B\left(\frac{55}{22}; 3\right) \\
 &\quad + \frac{9}{4}B\left(\frac{55}{22}; 4\right) + \frac{33}{28}B\left(\frac{55}{22}; 5\right) \\
 \Lambda^3\left(\frac{5}{2}\right) &= \frac{12}{35}B\left(\frac{55}{22}; 1\right) + \frac{33}{28}B\left(\frac{55}{22}; 2\right) + \frac{289}{180}B\left(\frac{55}{22}; 3\right) \\
 &\quad + \frac{23}{28}B\left(\frac{55}{22}; 4\right) + \frac{517}{252}B\left(\frac{55}{22}; 5\right) \\
 \Lambda^4\left(\frac{5}{2}\right) &= \frac{4}{7}B\left(\frac{55}{22}; 1\right) + \frac{5}{4}B\left(\frac{55}{22}; 2\right) + \frac{23}{36}B\left(\frac{55}{22}; 3\right) \\
 &\quad + \frac{7}{4}B\left(\frac{55}{22}; 4\right) + \frac{451}{252}B\left(\frac{55}{22}; 5\right) \\
 \Lambda^5\left(\frac{5}{2}\right) &= \frac{6}{7}B\left(\frac{55}{22}; 1\right) + \frac{15}{28}B\left(\frac{55}{22}; 2\right) + \frac{47}{36}B\left(\frac{55}{22}; 3\right) \\
 &\quad + \frac{41}{28}B\left(\frac{55}{22}; 4\right) + \frac{463}{252}B\left(\frac{55}{22}; 5\right). \tag{A.1}
 \end{aligned}$$

Also we report explicit expressions of the transfer cross sections between $J = 3/2, 5/2$ states:

$$\begin{aligned}
 \sigma^0\left(\frac{3}{2} \rightarrow \frac{5}{2}\right) &= \frac{1}{2\sqrt{6}}\left[3B\left(\frac{53}{22}; 1\right) + 5B\left(\frac{53}{22}; 2\right) + 7B\left(\frac{53}{22}; 3\right) \right. \\
 &\quad \left. + 9B\left(\frac{53}{22}; 4\right)\right]
 \end{aligned}$$

$$\begin{aligned}
 \sigma^1\left(\frac{3}{2} \rightarrow \frac{5}{2}\right) &= \frac{1}{2\sqrt{14}}\left[\frac{21}{5}B\left(\frac{53}{22}; 1\right) + \frac{13}{3}B\left(\frac{53}{22}; 2\right) \right. \\
 &\quad \left. + \frac{7}{15}B\left(\frac{53}{22}; 3\right) - 9B\left(\frac{53}{22}; 4\right)\right] \\
 \sigma^2\left(\frac{3}{2} \rightarrow \frac{5}{2}\right) &= \frac{1}{2\sqrt{21}}\left[\frac{21}{5}B\left(\frac{53}{22}; 1\right) - B\left(\frac{53}{22}; 2\right) \right. \\
 &\quad \left. - \frac{77}{10}B\left(\frac{53}{22}; 3\right) + \frac{9}{2}B\left(\frac{53}{22}; 4\right)\right] \\
 \sigma^3\left(\frac{3}{2} \rightarrow \frac{5}{2}\right) &= \frac{3}{10}B\left(\frac{53}{22}; 1\right) - \frac{9}{14}B\left(\frac{53}{22}; 2\right) + \frac{1}{5}B\left(\frac{53}{22}; 3\right) \\
 &\quad - \frac{3}{28}B\left(\frac{53}{22}; 4\right) \\
 \sigma^4\left(\frac{3}{2} \rightarrow \frac{5}{2}\right) &= 0. \tag{A.2}
 \end{aligned}$$

The usual fine structure transfer cross sections are:

$$\begin{aligned}
 \sigma\left(\frac{3}{2} \rightarrow \frac{5}{2}\right) &= \frac{1}{4}\left[3B\left(\frac{53}{22}; 1\right) + 5B\left(\frac{53}{22}; 2\right) \right. \\
 &\quad \left. + 7B\left(\frac{53}{22}; 3\right) + 9B\left(\frac{53}{22}; 4\right)\right] \\
 \sigma\left(\frac{5}{2} \rightarrow \frac{3}{2}\right) &= \frac{1}{4}\left[3B\left(\frac{35}{22}; 1\right) + 5B\left(\frac{35}{22}; 2\right) \right. \\
 &\quad \left. + 7B\left(\frac{35}{22}; 3\right) + 9B\left(\frac{35}{22}; 4\right)\right]. \tag{A.3}
 \end{aligned}$$

These cross sections are proportional to $\sigma^0(\frac{3}{2} \rightarrow \frac{5}{2})$.

See Paper II for the transfer cross sections formulae pertaining to $J = 1/2, 3/2$ states and (Kerkeni 2001) for explicit expressions of the Λ^κ in terms of the Zeeman cross sections for $J = 1/2, 3/2$ and $J = 5/2$ states.

References

- Blum, K. 1981, *Density Matrix Theory and Applications* (New York, London: Plenum Press)
- Casini, R., Landi Degl'Innocenti, E., Landolfi, M., & Trujillo Bueno, J. 2002, *ApJ*, 573, 864
- Czuchaj, E., Krosnicki, M., & Stoll, H. 2000, *Mol. Phys.*, 98, 419
- Dittmann, O., Trujillo Bueno, J., Semel, M., & López Ariste, A. 2001, in *Advanced Solar Polarimetry: Theory, Observation, and Instrumentation*, ed. M. Sigwarth, ASP Conf. Ser., 236, 125
- Dunning, T. H. 1989, *J. Chem. Phys.*, 90, 1007
- Fano, U. 1949, *J. Opt. Soc. Am.*, 39, 859
- Fano, U. 1954, *Phys. Rev.*, 93, 121
- Fano, U. 1957, *Rev. Mod. Phys.*, 29, 74
- Fano, U. 1963, *Phys. Rev.*, 131, 259
- Fuentealba, P., Von Szentpaly, L., Preuss, H., & Stoll, H. 1985, *J. Phys. B: Atom. Mol. Phys.*, 18, 1287
- Gandorfer, A. 2000, *The Second Solar Spectrum: A high spectral resolution polarimetric survey of scattering polarization at the solar limb in graphical representation*, vol. 1: 4625 Å to 6995 Å (Hochschulverlag AG an der ETH Zurich)
- Gandorfer, A. 2002, *The Second Solar Spectrum: A high spectral resolution polarimetric survey of scattering polarization at the solar limb in graphical representation*, vol. 2: 3910 Å to 4630 Å (Hochschulverlag AG an der ETH Zurich)
- Johnson, B.-R. 1977, *J. Chem. Phys.*, 67, 4086

- Kerkeni, B., Spielfiedel, A., & Feautrier, N. 2000, *A&A*, 358, 373
Erratum: 2000, *A&A*, 364, 937
- Kerkeni, B. 2001, Thèse de doctorat, Paris VI University
- Kerkeni, B. 2002, *A&A*, 390, 783
- Kerkeni, B., & Bommier, V. 2002, *A&A*, 394, 707
- Lamb, F. K., & ter Haar, D. 1971, *Phys. Rep.*, 2C, 253
- Landi Degl'Innocenti, E. 1998, *Nature*, 392, 256
- Landi Degl'Innocenti, E. 1999, in *Solar polarization*, ed. K. N. Nagendra, & J. O. Stenflo (Kluwer Academic Publishers), 61
- Launay, J. M., Roueff, E. 1977, *J. Phys. B: Atom. Molec. Phys.*, 10, 879
- Leininger, T., Gadéa, F. X., & Dickinson, A. S. 2000, *J. Phys. B: Atom. Molec. Opt. Phys.*, 33, 1805
- Manso Sainz, R., & Trujillo Bueno, J. 2001, in *Advanced Solar Polarimetry: Theory, Observation, and Instrumentation*, ed. M. Sigwarth, ASP Conf. Ser., 236, 213
- Manso Sainz, R., & Landi Degl'Innocenti, E. 2002, *A&A*, 394, 1093
- Mc Farland, R. H., Schlachter, A. S., Stearns, J. W., Liu, B., & Olson, R. E. 1982, *Phys. Rev. A*, 26, 775
- Mies, F. H. 1973, *Phys. Rev. A*, 7, 942
- Monteiro, T. S., Danby, G., Cooper, I. L., Dickinson, A. S., & Lewis, E. L. 1988, *J. Phys. B: Atom. Molec. Phys.*, 21, 4165
- Müller, W., Flesh, J., & Meyer, J. 1984, *J. Chem. Phys.*, 80, 3297
- Nienhuis, G. 1976, *J. Phys. B: Atom. Molec. Phys.*, 9, 167
- Omont, A. 1977, *Prog. Quantum Electronics*, 5, 69
- Reid, R. H. G. 1973, *J. Phys. B: Atom. Molec. Phys.*, 6, 2018
- Spielfiedel, A., Feautrier, N., Chambaud, G., & Lévy, B. 1991, *J. Phys. B: Atom. Molec. Phys.*, 24, 4711
- Stenflo, J. O., & Keller, C. 1997, *A&A*, 321, 927
- Stenflo, J. O., Keller, C., & Gandorfer, A. 2000, *A&A*, 355, 789
- Stenflo, J. O. 2001, in *Advanced Solar Polarimetry: Theory, Observation, and Instrumentation*, ed. M. Sigwarth (San Francisco: Astronomical Society of the Pacific), ASP Conf. Ser., 236, 97
- Trujillo Bueno, J., & Landi Degl'Innocenti, E. 1997, *ApJ*, 482, L183
- Trujillo Bueno, J. 1999, in *Solar polarization Astrophysics and Space Science Library* (Dordrecht: Kluwer Academic Publishers), ed. K. N. Nagendra, & J. O. Stenflo, vol. 243, 73
- Trujillo Bueno, J. 2001, in *Advanced Solar Polarimetry: Theory, Observation, and Instrumentation*, ed. M. Sigwarth, ASP Conf. Ser., 236, 161
- Trujillo Bueno, J., & Manso Sainz, R. 2001, in *Magnetic Fields Across the Hertzsprung-Russell Diagram*, ed. G. Mathys, S. K. Solanki, & D. T. Wickramasinghe (San Francisco: Astronomical Society of the Pacific), ASP Conf. Ser., 248, 83
- Trujillo Bueno, J., Landi Degl'Innocenti, E., Collados, M., Merenda, L., & Manso Sainz, R. 2002a, *Nature*, 415, 403
- Trujillo Bueno, J., Casini, R., Landolfi, M., & Landi Degl'Innocenti, E. 2002b, *ApJ*, 566, L53